

# Determination of microscopic residual stresses using evolutionary algorithms

J. Ignacio Hidalgo

Universidad Complutense de Madrid  
Madrid, Spain  
hidalgo@ucm.es

Ricardo Fernández

Centro Nacional de Investigaciones  
Metalúrgicas, CENIM, CSIC  
Madrid, Spain  
ric@cnim.csic.es

J, Manuel Colmenar

Universidad Rey Juan Carlos  
Móstoles, Madrid, Spain  
josemanuel.colmenar@urjc.es

Oscar Garnica

Universidad Complutense de Madrid  
Madrid, Spain  
ogarnica@ucm.es

Juan Lanchares

Universidad Complutense de Madrid  
Madrid, Spain  
julandan@ucm.es

Gaspar González-Doncel

Centro Nacional de Investigaciones  
Metalúrgicas, CENIM, CSIC  
Madrid, Spain  
ggd@cnim.es

## ABSTRACT

Residual stresses, both macroscopic and microscopic, are originated during conventional metallurgical processes. Knowing their magnitude and distribution is of great importance in the structural design of applications where fatigue, stress corrosion or thermal cycling occur (e.g., in the aerospace industry). The importance of these stresses is reflected in the large number of articles published in recent years, mainly focused on studying macroscopic stresses. However, there are no experimental studies that quantify the magnitude of microscopic triaxial stresses. This lack is due in part to the limitations of diffraction techniques (neutrons and synchrotron radiation). Since the measurement volume is much higher than the variation of these microscopic stresses, its calculation is greatly complicated, because the methods used in the case of macroscopic stresses are not valid for microscopic ones. Furthermore, there is no reliable procedure to obtain the relaxed lattice parameter value, a key factor in the calculation of residual stresses. The aim of this paper is to present the main ideas oriented to develop a methodology for mapping microscopic stresses, particularly in aluminium alloys such as those commonly used in the aerospace industry. The procedure will use experimental diffraction results obtained from large European facilities, mainly by neutron diffraction. This information will be analyzed using evolutionary algorithms, computational techniques that handle a large number of variables. The procedure will be based on the analysis of the shift of the diffraction peaks and, fundamentally, their broadening. For simplicity, non-heat treatable alloys will be used as they do not experience lattice parameter variation with heat treatments.

---

Permission to make digital or hard copies of all or part of this work for personal or classroom use is granted without fee provided that copies are not made or distributed for profit or commercial advantage and that copies bear this notice and the full citation on the first page. Copyrights for components of this work owned by others than the author(s) must be honored. Abstracting with credit is permitted. To copy otherwise, or republish, to post on servers or to redistribute to lists, requires prior specific permission and/or a fee. Request permissions from [permissions@acm.org](mailto:permissions@acm.org).

GECCO '19, July 13–17, 2019, Prague, Czech Republic

© 2019 Copyright held by the owner/author(s). Publication rights licensed to the Association for Computing Machinery.

ACM ISBN 978-1-4503-6748-6/19/07...\$15.00

<https://doi.org/10.1145/3319619.3326824>

## CCS CONCEPTS

• **Computing methodologies** → **Search methodologies**; • **Applied computing** → **Physical sciences and engineering**; • **Applied computing** → *Aerospace*;

## KEYWORDS

Aluminium alloys, Neutron diffraction, Multi-objective optimization, EBSD maps

### ACM Reference Format:

J. Ignacio Hidalgo, Ricardo Fernández, J, Manuel Colmenar, Oscar Garnica, Juan Lanchares, and Gaspar González-Doncel. 2019. Determination of microscopic residual stresses using evolutionary algorithms. In *Proceedings of the Genetic and Evolutionary Computation Conference 2019 (GECCO '19)*. ACM, New York, NY, USA, 7 pages. <https://doi.org/10.1145/3319619.3326824>

## 1 INTRODUCTION

Periodically, mass media report about accidents at industrial facilities, oil platforms, factories, etc. Accidents such as bursting pipes, fuel tanks or large vessels collapsing due to corrosion or fatigue problems, and failures in various components which, before the end of the planned life cycle, fail suddenly and sometimes tragically. Those news usually do not focus on the technical details of the accident or its causes. Attention is mainly focused on the economic cost involved and, fundamentally, on the human factor; the people involved, injured or dead. Usually, there is a technical question behind the accident, such a bad design, an inadequate selection of the material. Undoubtedly, the detailed analysis of these faults and the knowledge of their cause has served to advance in new designs and to improve the performance of new components, in particular in the aerospace sector where problems associated with fatigue behavior are critical. These analyses are often complex and not always accurate. A reliable diagnosis requires a whole history of data on materials, their conditions of use, their microstructural characteristics, etc., information that is not always available. Therefore, it is common to resort to tolerance margins that alleviate the ignorance of these factors in anticipation of their possible relevance during the service life of the component.

This is the area where the residual stresses are found. These stresses are generally present in materials and components. They

are originated in the different stages of their manufacturing process. In the aerospace industry, for example, understanding in depth the development (and control) of residual stresses would improve the performance of components. It is believed that these stresses are critical in the development and progression of cracks during fatigue behavior.

Whenever there is a non-homogeneous dimensional change (deformations and/or expansions), residual stresses are generated. In the case of macroscopic stresses, they can be determined without great complexity, but there are other stresses, the microscopic ones, whose magnitude is still unknown. However, their influence on the problems described may also be relevant. This project is focused on determining these microscopic stresses. Specifically, an attempt will be made to develop a procedure for mapping these microscopic stresses for structural materials, e.g., alloys used in the aerospace industry.

This workshop paper describes the preliminary ideas of a project that is being developed under the collaboration of two research groups. The purpose is to participate in the workshop to get ideas from the evolutionary computation community to address the problem. In section 2 we explain the different residual stresses that can appear in materials. Section 3 summarizes our previous work in this area, where evolutionary algorithms were developed to solve a similar problem, in this case focused in determining macroscopic residual stresses. Finally, in Section 4 we explain the initial proposal of the project.

## 2 RESIDUAL STRESSES IN MATERIALS

The different residual stresses in materials [9] are distinguished in the dimensional scale in which they vary. Although this scale differs by orders of magnitude, its amplitude, however, is not necessarily very different, Figure 1. In a first approximation, these stresses are divided into macroscopic and microscopic.

The origin of the first ones, type I stresses or M-RS, can be understood from a description of the materials as continuum media. They result from a very local thermomechanical process during the manufacture of a given component (e.g., a welding process). These stresses are determined by means of diffraction methods using penetrating radiation (neutrons or synchrotron x-ray radiation) [8]. Inasmuch they are penetrating radiations, they allow the triaxial stress state to be resolved in a non-destructive manner. The calculation of this stress is carried out by having a relaxed value,  $d^0$ , of the lattice spacing of a given  $hkl$  plane, which is used as a reference to measure the strains in different regions of the sample. The key factor is that this probe is usually a gauge volume of few  $mm^3$ , that is, it size is significantly smaller than the variation of the macroscopic stress. It is assumed that the deformation that takes place in this volume is well represented by the expansion/contraction of the lattice spacing of the selected  $hkl$ .

To determine macroscopic stresses, the displacement,  $d$ , of the diffraction peaks with respect to  $d^0$  is analyzed (see Figure 2. In this way, the elastic deformation in this gauge volume is calculated using the same equation employed to calculate the elastic deformation in a tensile test (equation 1):

$$\epsilon_l = \frac{d_{hkl} - d_{hkl}^0}{d_{hkl}^0} \quad (1)$$

Using the linear elasticity (generalized Hooke's Law), the stress associated with this deformation is calculated. Since the technique is non-destructive and allows the triaxial state to be calculated, it has led to a great progress in the determination of residual stresses in components with respect to conventional techniques (blind hole, etc.). The fact that only peak shift is used in the analysis makes the calculation of stresses a relatively easy task

To understand the origin of microscopic stresses, or m-RS, however, it is necessary to invoke the microstructure of materials. These stresses are classified into two types, microscopic stresses, also called intergranular stresses, (type II) and intragranular stresses (type III), Figure 1. The microscopic stresses of type II (or mRS), which are of interest in this research, vary among neighboring grains, Figure 1, as a consequence of the different degree of plastic (and elastic) deformation that a grain has undergone with respect to its neighbors during a given metallurgical process (e.g., rolling). Microscopic intragranular stresses (type III) are associated with distortions of the crystalline lattice, at a very local level, within a given grain. They are associated with the presence of lattice defects: dislocations, precipitates, solute/interstitial atoms, etc., Figures 1 and 2. Like type II, their amplitude can be comparable to macroscopic stresses, and even exceed them. These stresses cannot be studied using the methods that will be employed in this project and, therefore, will not be treated here. The diffraction techniques used to calculate macroscopic stresses also reveal, although in a different way, the presence of microscopic stresses. Since the gauge volume is much larger than the grain size and these have different stresses, the effect on the diffraction peaks is more complex: they undergo shift and broadening, Figure 2. This circumstance makes it extremely difficult to calculate the stresses of individual grains to the extent that it has not yet been possible to map the triaxial state of type II stresses. Some attempts have been made by means of EBSD, from the changes or distortions that are produced in the Kikuchi lines as a consequence of a stress state. However, these changes only give a qualitative idea of the stresses in a grain: but not a rigorous description of its stress tensor [6, 7]. It is important to highlight the limitations of the EBSD technique to achieve the objective of this research. Although relevant work has been carried out in recent years that account for important studies on microscopic stresses, e.g., such as those of A.J. Wilkinson's group at the University of Oxford [1, 4], the fact that the relaxed value,  $d^0$ , is unknown makes the desired task impossible. In addition, there is always the limitation implied by the fact that it is not possible to calculate the triaxial state of stresses of the different grains (equation 1) while the measurement is superficial, so that the stress state of the grains in these circumstances is always biaxial. The EBSD technique, however, in combination with x-ray macrotexture, will be essential in this study to determine the crystallographic orientation of individual grains which stresses are intended to be calculated.

## 3 EVOLUTIONARY ALGORITHMS TO DETERMINE THE RESIDUAL STRESS

An analysis of the unstressed lattice spacing,  $d^0$ , for the determination of the residual stress profile (M-RS) in a friction stir welded (FSW) 10 mm thickness plate of an age-hardenable AA2024 aluminum alloy has been completed through the use of a genetic

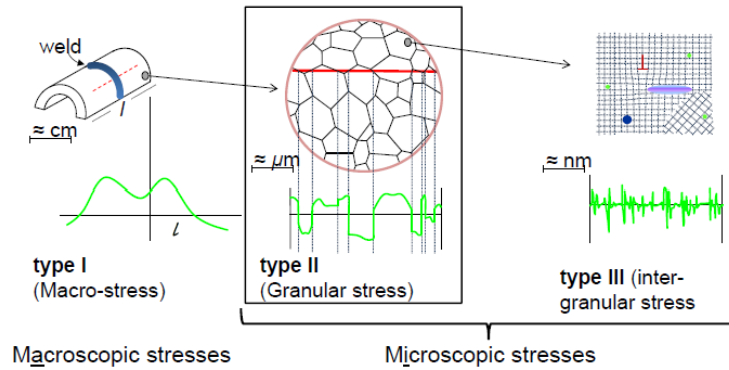


Figure 1: Diagram of the three types of residual stresses and the scale on which each of them varies. Intergranular microscopic stresses, type II, are of interest in this research. Their oscillation is linked to the grain size, which can reach the nanometric scale.

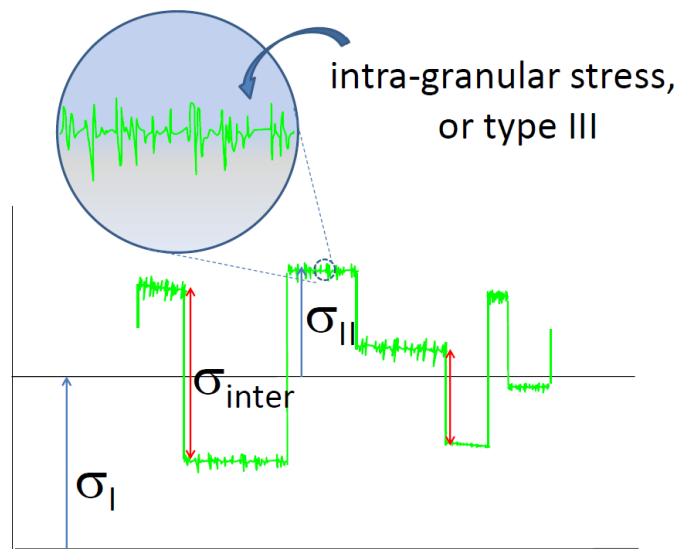


Figure 2: Effect of residual stresses on the diffraction peak: type I stresses cause peak shift, type II stresses also cause broadening due to the fact that the grains have different stresses. b) Contributions to the total residual stress. The difference between the microscopic stress in a grain,  $\sigma_{II}$ , and that of its neighbor is the inter-granular stress,  $\sigma_{INTER}$ , itself ( $\sigma_{INTER}$ , is shown by the red arrows).  $\sigma_I$  is the macroscopic residual stress in a specific region of the sample

algorithm [2, 5]. Procedures based on equilibrium conditions (stress and bending moment) were used to obtain an un-stressed lattice spacing,  $d^0$ , as a crucial requirement for calculating the residual stress (RS) profile across the welded joint. Two procedures have been used that take advantage of neutron diffraction measurements.

First, equilibrium conditions were imposed on sections parallel to the weld so that a constant  $d^0$ , value corresponding to the base material region could be calculated analytically. Second, balance

conditions were imposed on a section transverse to the weld. Then, using the data and the genetic algorithm, suitable  $d^0$ , values for the different regions of the weld have been found. For several reasons, the comb method has proved to be inappropriate for RS determination in the case of age-hardenable alloys. However, the equilibrium conditions, together with the genetic algorithm, has been shown to be very suitable for determining the RS profiles in FSW joints of

these alloys, where inherent microstructural variations of  $d^0$  across the weld are expected.

Aircraft structures often use aluminium alloys from the AA2xxx series in the construction process. In fact, these materials have usually to be welded, which implies that a residual stress (RS) is developed. In order to calculate the RS profile across the weld of aluminium alloy AA2024 it is required to know the un-stressed lattice spacing,  $d^0$ , which depends on the amount of alloying elements, such as copper atoms, across the weld. Therefore, since the heat treatment across the weld is not uniform, the amount of solute atoms is different leading to different  $d^0$  values. This reveals that the conventional analytical procedures are not applicable since  $d^0$  is not constant.

In [5], an evolutionary algorithm was proposed to estimate the  $d^0$  values under three different scenarios which correspond to different sample sizes. For each scenario, nine parameters are required, corresponding to three depths across the thickness of the plate (front, center and back) and the three stress components (L, N and T). However, the same  $d^0$  value is obtained irrespective of the sample direction. Hence, only 3 parameters are used for each zone:  $d_{zone_i}^{0LFront}$ ,  $d_{zone_i}^{0LCenter}$  and  $d_{zone_i}^{0LBack}$ .

As a consequence, the codification of the individuals in the algorithm is direct. Each gene stores the value of one parameter considering that the first three genes correspond to the first zone, the second group to the second zone, and so on. Hence, the chromosome length is  $3 \cdot n$ , where  $n$  is the number of zones in the sample, whose value depends on the selected scenario.

Physical experimentation allows to establish a threshold in the values of the  $d^0$  components. In particular, taking into account a precision of five decimal digits, it is known that, for each zone  $i$

$$1.22000 \cdot 10^{-15} < d_{zone_i}^0 < 1.22999 \cdot 10^{-15}$$

As a consequence, it is possible to use an integer codification where the values of the genes range from 0 to 999, decoding the value of each gene with the operation shown in Equation (2).

$$d_{zone_i}^0 = (1.22 + gene \cdot 10^{-5}) \cdot 10^{-15} \quad (2)$$

The research carried out in [5] consisted on a Multi-Objective Evolutionary Algorithm (MOEA) able to estimate the value of those parameters that define  $d^0$ . The two conflicting objective functions to minimize were the sum of the longitudinal stresses, calculated with Equation (3); and the bending moments in a transverse section of the welded plate, calculated with Equation (4). In both cases, if the algorithm reaches the value of 0, it will find the correct  $d^0$  values.

$$F_1 = T_{Front} + T_{Center} + T_{Back} \quad (3)$$

$$F_2 = T_{Front} - T_{Back} \quad (4)$$

The  $T_{Front}$ ,  $T_{Center}$  and  $T_{Back}$  components of the objective function equations correspond to the normal stress to each one of the front, center and back regions of the weld. Equation (5) shows the computation of  $T_{Front}$ , which makes use of several  $d^0$  components, as well as  $C_1$  and  $C_2$  which are constant values that depend on the particular alloy under study. Analogous equations are considered to calculate  $T_{Center}$  and  $T_{Back}$ .

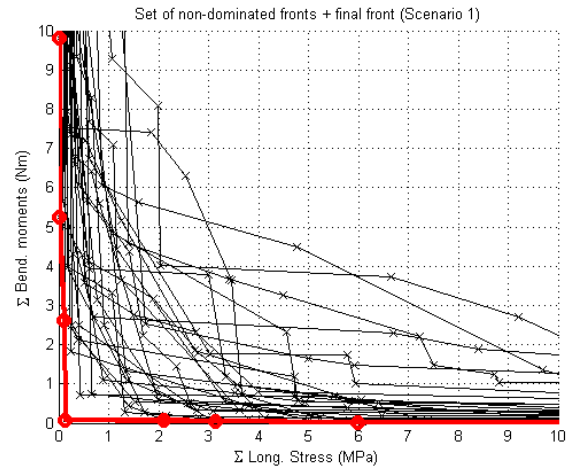


**Figure 3: Pareto fronts for the runs of Scenario 1. Red line shows the non-dominated solutions. Reprinted from [5] Copyright (2015), with permission from Elsevier.**

$$T_{Front} = \sum_{i=0}^z \left[ (C_1 + C_2) \cdot \frac{d_{311}^{Front}[i] - d_i^{0LFront}}{d_i^{0LFront}} + C_2 \cdot \left( \frac{d_{311}^{Center}[i] - d_i^{0LFront}}{d_i^{0LFront}} + \frac{d_{311}^{Back}[i] - d_i^{0LFront}}{d_i^{0LFront}} \right) \right] \quad (5)$$

The experimentation consisted on 30 runs of a NSGA-II algorithm [3] for each one of the scenarios. The initial population was randomly generated and 10000 generations were run over a population of 1000 individuals. The crossover and mutation probabilities were 0.8 and 0.1 respectively, while the selection of mates were performed with a binary tournament operator.

As explained before, three scenarios were considered in that work. Scenario 1 takes into account the smallest space of solutions because it uses at boundary values the maximum and minimum measurements made by the neutron diffraction experiment. Scenario 2 divides the sample into 181 points homogeneously distributed considering the same boundaries as Scenario 1, which leads to a faster and more effective search. In Scenario 3 the dimensions of the zones in the transverse section are known. Hence, it is possible to fix the boundaries not for the whole area, but for each one of the zones, reducing the search space in relation to the previous scenarios. There is an additional variant of this scenario, called Scenario 3b, where the value of  $d_{hkl}^0$  in the base material is also known.

Figures 3, 4, 5 and 6 show the Pareto fronts for the experiment on the four described scenarios, highlighting in red the non-dominated solutions among each experiment. As it can be seen in the Figures, the resulting values are very close to 0 in any of the objective functions. We refer the reader to [5] for the results regarding the performance of the algorithm in terms of hypervolume.

From the metallurgical point of view the results are very good. As an example, Figure 7 shows the measured hardness of the sample in comparison with the result obtained by one of the solutions in

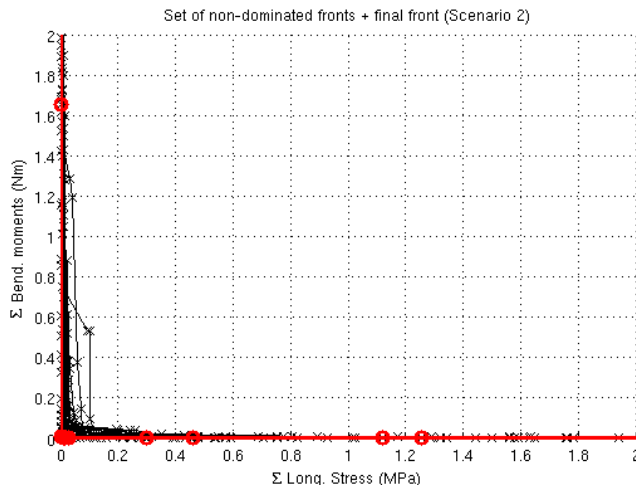


Figure 4: Pareto fronts for the runs of Scenario 2. Red line shows the non-dominated solutions. Reprinted from [5] Copyright (2015), with permission from Elsevier.

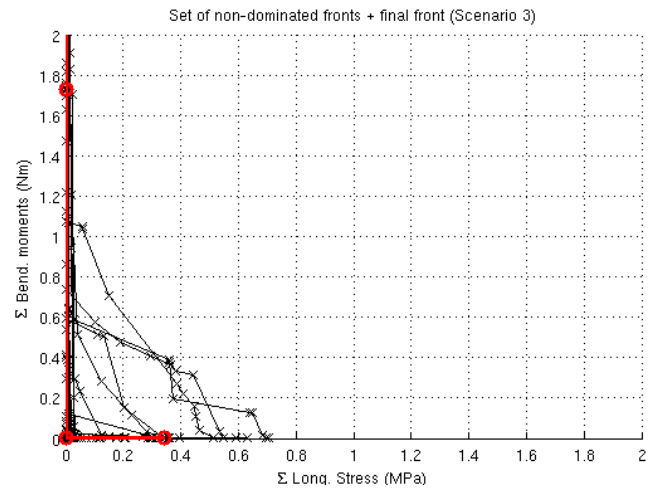


Figure 6: Pareto fronts for the runs of Scenario 3. Red line shows the non-dominated solutions. Reprinted from [5] Copyright (2015), with permission from Elsevier.

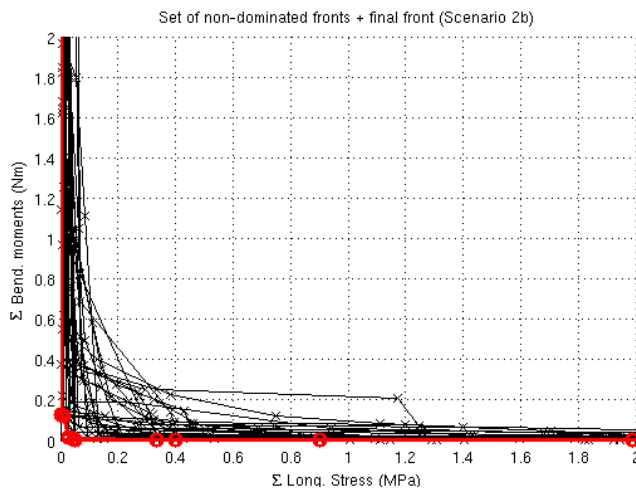


Figure 5: Pareto fronts for the runs of Scenario 3. Red line shows the non-dominated solutions. Reprinted from [5] Copyright (2015), with permission from Elsevier.

Scenario 3. As it can be seen in the figure, the shape is quite similar, revealed as the typical W form in this kind of models.

#### 4 PROPOSAL

The different residual stresses in materials [1] are distinguished in the dimensional scale in which they are manifested. Although this scale differs in orders of magnitude, its amplitude, however, is not necessarily very different. In a first approach, these stresses are, as mentioned above, divided into macroscopic and microscopic. In order to understand the origin of microscopic stresses, it is necessary to delve deeper into the microstructure of the materials. These microscopic stresses are classified into intergranular (type II) and intragranular (type III). The microscopic stresses of type II

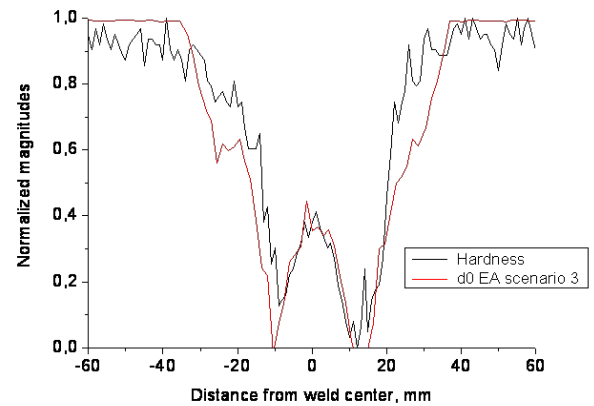
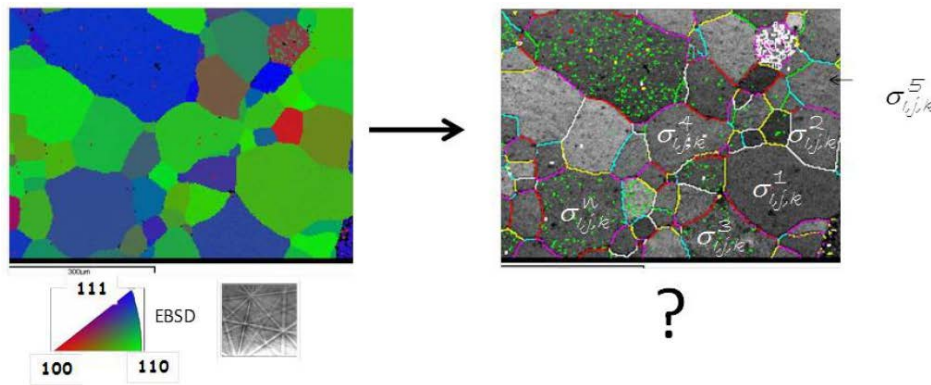


Figure 7: Normalized values of experimental hardness and EA  $d^0$  prediction. Reprinted from [5] Copyright (2015), with permission from Elsevier.

(or mRS), which are of interest in this research, vary among neighbouring grains, as a consequence of the different degree of plastic (and elastic) deformation that a grain undergoes with respect to its neighbors during a given metallurgical process (e.g., rolling).

The diffraction techniques used to calculate macroscopic stresses also reveal, albeit in different ways, the presence of microscopic stresses. Since the gauge volume is much larger than the grain size and these have different stresses, the effect on diffraction peaks is more complex as they experience not only a shift with respect the un-stressed position, but also broadening.

This circumstance entails an enormous difficulty in calculating the stresses of individual grains to the extent that it has not yet been possible to map the triaxial state of type II stresses. The EBSD



**Figure 8: Map of individual orientations of a microstructure and the equivalent map of residual stresses to be determined. The first one is obtained by means of EBSD. The second will require diffraction peak data and evolutionary algorithms, as proposed in the project.**

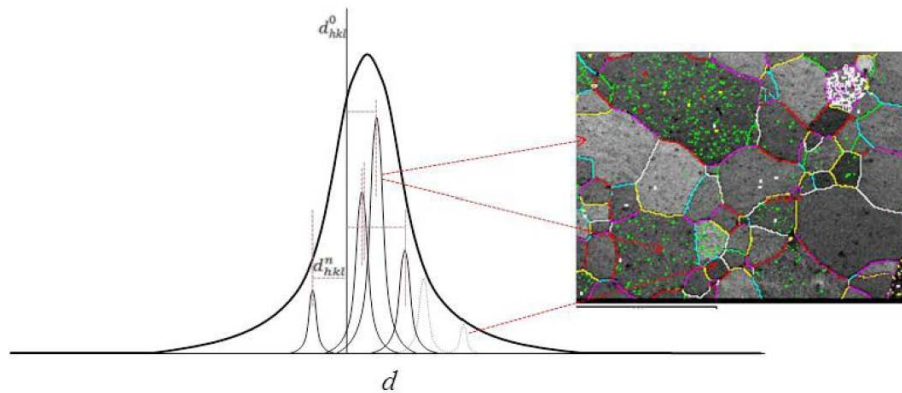


**Figure 9: Simplified description of the effect of the different stress of individual grains on the displacement and widening of the diffraction peak. Each peak is generated by a group of grains that have a given  $hkl$ , normal to the observation surface, but each grain has different stress.**

technique, based on back-scattered electrons, is the most convenient one for the study of micro-texture or the determination of the individual orientations of a significant number of crystalline grains. Some attempts have been made using EBSD maps, from the changes or distortions that occur in the Kikuchi lines as a result of a stress state, but the resulting stress calculated can only be limited to 2D. The EBSD technique, however, will be essential in this study to determine the crystallographic orientation of the grain map whose stresses are being estimated. Both, macro- and micro-texture studies will be essential to finally determine the 3D stress state of individual grains

The method proposed in this research will try to obtain the stress map of a number of grains from microstructures of aluminum alloys from which metallographic images will be obtained. It is proposed to work first on a sample extracted from an extrusion process, which gives rise to a known symmetry in the microstructure, higher than in other processes such as rolling. A cylinder, extracted from an extruded bar, will be machined and subjected to a heating process

(to about 530 °C) followed by water quenching. This will generate microscopic (and macroscopic) stresses that we intend to investigate. Figure 8 summarises the way in which this objective is to be achieved. From the information that will be obtained through EBSD of the grain orientations of a microstructure and through the data of the diffraction peaks, Figure 9, the corresponding map of the triaxial state of the stresses of individual grains will be established. The use of evolutionary algorithms will be the tool that enables this analysis given its ability to handle a large number of variables. Figure 9 reveals the effect that the different stress state of individual grains provokes on the diffraction peaks; both, shift and broadening of a specific diffraction peak occurs. It is important to note that these grains possess the common  $hkl$  reflection for a given sample direction. For simplicity, non-heat-teatable, aluminum alloys will be selected to avoid the problems associated with the variation of  $d^0$  with the amount of alloying elements; i.e., precipitation. In these alloys, heat treatment do not change the amount of solid solution atoms.

From the EBSD images of the micro structure we will obtain the following information:

- The number, size and aspect ratio of the grains. We will work with homogeneous structures, with the purpose of assuming only one size for all the grains.
- The macroscopic texture to establish the preferential orientations of the grains.
- The map of individual orientations of the grains of these microstructures. With this, it will be possible to associate diffraction peaks of a specific  $hkl$  to specific grain collectives. The microtexture maps obtained by EBSD must agree with the macrotexture measurements.

The essential information, which will be used to calculate the microscopic stress state of the grains, is not only in the position of the diffraction peaks (shift) but also in their width. That is to say, in their differences with respect to the grain diffraction peaks of the un-stressed sample. The diffraction peaks to be studied will be obtained from different experiments in Large Facilities; preferably neutron sources (ILL, IBRII), as explained above. To this end, proposals will be sent according to the procedures for the access to these instruments. We will work with samples with microscopic stresses and un-stressed samples in order to have a reference. For this purpose, a sample will be annealed (at some 530 °C) and, subsequently, quenched to develop the RS fields. Another sample will be, instead, furnace cooled (from the annealing temperature) to obtain an un-stressed reference sample. To ensure a relaxed  $d_0$  value, also powders treated a high temperature to relax stresses, will be used in the diffraction experiment. Obviously, diffraction experiments cannot be performed with the samples that will be used for the metallographic study to obtain the images of the microstructures and the EBSD maps. It is therefore important to use materials with homogeneous and representative microstructures. It must be ensured that the microstructure of samples for metallography is similar to that of samples for diffraction experiments. In other words, we will work on the hypothesis that if it were possible to do the diffraction experiments in the specific microstructures on which the microscopy and micro- and macro-texture studies were performed, we would obtain identical peaks to those that will be obtained in the samples for diffraction. With this information, which contains a large number of variables, it should be possible to determine the triaxial state of the individual grains, Figure 9, given appropriate assumptions. The objective is to obtain the stress tensor of each of the grains, which supposes 3000 variables for a microstructure with 1000 grains.

The calculation or search process will consist of relating each of the diffraction peaks obtained in each direction of the sample with those grains favorably oriented. The critical step focuses on the computational algorithm which, if the input hypothesis is correct, must allow the reconstruction of the diffraction peaks to which the favorably oriented grains give rise in each case. This will be achieved by carrying out a search that will consist of reconstructing the diffraction peaks corresponding to different stress states until the one that "reproduces" the peaks obtained experimentally

is found, Figures 8 and 9. Given the high number of parameters and their possible ranges of values, derived from the also high number of possible stress states, the size of the search space that the algorithm will have to handle is extremely large. This enormous size prevents the use of deterministic algorithmic techniques, since their execution time would be unaffordable. In this type of problems with such large search spaces, algorithmic techniques based on metaheuristics enable acceptable solutions to be found in affordable execution times. The search will be carried out assuming a known  $d^0$ . This information will be possible given the fact that diffraction peaks from an un-stressed sample will be also obtained in the experiments. In addition, it must comply with a stress state resulting after conventional equilibrium condition of forces are imposed, both at the macro- and microscopic scales, of grains that meets certain conditions of mechanical equilibrium at the microscopic level. As mentioned above, these algorithms have already successfully solved the problem addressed by this group of the macroscopic stress state across a welded plate of an age-hardenable aluminum alloy [2, 5], as explained in Section 3.

## ACKNOWLEDGMENTS

The work is supported by the synergistic R&D projects in new and emerging scientific areas at the frontier of science and of an interdisciplinary nature, co-financed by the Operational Programs of the European Social Fund and the European Development Regional Fund, 2014-2020, of the government of Madrid, Project Y2018/NMT-4668 (Micro-Stress- MAP-CM), Project GenObIA-CM (S2017 / BMD-3773) financed by the Community of Madrid and co-financed with EU Structural Funds and Fundación Eugenio Rodríguez Pascual grants.

## REFERENCES

- [1] Hamidreza Abdolvand and Angus J Wilkinson. 2016. Assessment of residual stress fields at deformation twin tips and the surrounding environments. *Acta Materialia* 105 (2016), 219–231.
- [2] F Cioffi, JI Hidalgo, Ricardo Fernández, T Pirling, B Fernández, D Gestó, I Puente Orench, Pilar Rey, and Gaspar González-Doncel. 2014. Analysis of the unstressed lattice spacing,  $d_0$ , for the determination of the residual stress in a friction stir welded plate of an age-hardenable aluminum alloy—Use of equilibrium conditions and a genetic algorithm. *Acta Materialia* 74 (2014), 189–199.
- [3] Kalyanmoy Deb, Amrit Pratap, Sameer Agarwal, and T. Meyarivan. 2002. A Fast and Elitist Multiobjective Genetic Algorithm: NSGA-II. *IEEE Trans. Evolutionary Computation* 6, 2 (2002), 182–197.
- [4] Y Guo, H Abdolvand, TB Britton, and AJ Wilkinson. 2017. Growth of  $\{112\ 2\}$  twins in titanium: A combined experimental and modelling investigation of the local state of deformation. *Acta Materialia* 126 (2017), 221–235.
- [5] J Ignacio Hidalgo, Ricardo Fernández, J Manuel Colmenar, Florencia Cioffi, José L Risco-Martín, and Gaspar González-Doncel. 2016. Using evolutionary algorithms to determine the residual stress profile across welds of age-hardenable aluminum alloys. *Applied Soft Computing* 40 (2016), 429–438.
- [6] Mehmet E Kartal, Fionn PE Dunne, and Angus J Wilkinson. 2012. Determination of the complete microscale residual stress tensor at a subsurface carbide particle in a single-crystal superalloy from free-surface EBSD. *Acta materialia* 60, 13-14 (2012), 5300–5310.
- [7] T Okada, X Huang, K Kashihara, F Inoko, and JA Wert. 2003. Crystal orientations before and after annealing in an Al single crystal strained in tension. *Acta materialia* 51, 7 (2003), 1827–1839.
- [8] Philip J Withers and HKDH Bhadeshia. 2001. Residual stress. Part 1—measurement techniques. *Materials science and Technology* 17, 4 (2001), 355–365.
- [9] Philip J Withers and HKDH Bhadeshia. 2001. Residual stress. Part 2—Nature and origins. *Materials science and technology* 17, 4 (2001), 366–375.